

Collective-coupling analysis of spectra of mass-7 isobars: ${}^7\text{He}$, ${}^7\text{Li}$, ${}^7\text{Be}$, ${}^7\text{B}$.

L. Canton^{(1),*} G. Pisent^{(1),†} K. Amos^{(2),‡} S. Karataglidis^{(2,3),§} J. P. Svenne^{(4),¶} and D. van der Knijff^{(5)**}

⁽¹⁾*Istituto Nazionale di Fisica Nucleare, sezione di Padova, e Dipartimento di Fisica dell'Università di Padova, via Marzolo 8, Padova I-35131, Italia*

⁽²⁾*School of Physics, University of Melbourne, Victoria 3010, Australia*

⁽³⁾*Department of Physics and Electronics, Rhodes University, Grahamstown 6140, South Africa*

⁽⁴⁾*Department of Physics and Astronomy, University of Manitoba, and Winnipeg Institute for Theoretical Physics, Winnipeg, Manitoba, Canada R3T 2N2 and*

⁽⁵⁾*Advanced Research Computing, Information Division, University of Melbourne, Victoria 3010, Australia*

(Dated: today)

Abstract

A nucleon-nucleus interaction model has been applied to ascertain the underlying character of the negative-parity spectra of four isobars of mass seven, from neutron- to proton-emitter driplines. With one and the same nuclear potential defined by a simple coupled-channel model, a multichannel algebraic scattering approach (MCAS) has been used to determine the bound and resonant spectra of the four nuclides, of which ${}^7\text{He}$ and ${}^7\text{B}$ are particle unstable. Incorporation of Pauli blocking in the model enables a description of all known spin-parity states of the mass-7 isobars. We have also obtained spectra of similar quality by using a large space no-core shell model. Additionally, we have studied ${}^7\text{Li}$ and ${}^7\text{Be}$ using a dicluster model. We have found a dicluster-model potential that can reproduce the lowest four states of the two nuclei, as well as the relevant low-energy elastic scattering cross sections. But, with this model, the rest of the energy spectra cannot be obtained.

PACS numbers: 24.10-i;25.40.Dn;25.40.Ny;28.20.Cz

*Electronic address: luciano.canton@pd.infn.it

†Electronic address: pisent@pd.infn.it

‡Electronic address: amos@physics.unimelb.edu.au

§Electronic address: s.karataglidis@ru.ac.za

¶Electronic address: svenne@physics.umanitoba.ca

**Electronic address: dirk@unimelb.edu.au

I. INTRODUCTION

Currently there is much interest in the structure of, and reactions with, radioactive nuclei. In particular, attention has been given to weakly-bound light nuclei, which may manifest exotic structure. The very extended neutron matter distributions of ${}^6\text{He}$ and ${}^{11}\text{Li}$ that have been called neutron halos are examples. They contrast with ${}^8\text{He}$ and ${}^9\text{Li}$ which have neutron skins. Signatures of those neutron matter distributions have been noted in the cross sections from elastic and inelastic scattering of the nuclei from hydrogen [1, 2]. As yet, relatively few such experiments have been made (elastic and inelastic scattering of radioactive ion beams (RIB) from a hydrogen target). We hope that will change in the near future, since appropriate scattering theories to describe the events not only exist but also have been implemented [2, 3]. Most of the existing RIB-hydrogen scattering data have been taken with ions of medium energies, analyses of which are appropriately made using a g -folding model of the optical potential for elastic scattering and a distorted wave approximation (DWA) analysis of inelastic scattering data [4]. For low energies, however, a coupled-channel theory is more relevant. Then the MCAS method [3] is a most appropriate way to proceed.

Low energy nucleus-nucleon scattering data exhibit resonances, analyses of which reflect structure of the compound nucleus formed by the ion and proton target. Such was described in a recent publication [5]. Also MCAS analyses of data from the scattering of low energy ${}^{14}\text{O}$ ions from hydrogen [6] revealed that the spectrum should have a number of narrow resonances at energies slightly higher than the observed two broad resonances that coincide with the ground and first excited states of the proton-unstable ${}^{15}\text{F}$. The centroids, widths, and spin-parity assignments all are determined using the MCAS approach [5].

Herein we use the MCAS theory for the interactions of ${}^6\text{He}$ and of ${}^6\text{Be}$ with nucleons. The spectrum of ${}^7\text{Li}$ is used to set that matrix of potentials. Thereafter with the interaction held fixed, we predict the spectra of the other mass-7 isobars, of which ${}^7\text{He}$ and ${}^7\text{B}$ are particle unstable. The MCAS method [3] appears particularly suited to this problem in that it describes the bound and resonant spectra of even-odd light nuclei in terms of nucleon-nucleus dynamics in the context of coupled-channel interactions. Even a simplistic collective model, with geometric-type deformation for the structure of the nucleus, can give a very reasonable description of the compound system [7]. That is so only if the non-local effects of Pauli blocking are taken into account in the nucleon-nucleus model Hamiltonian. With MCAS, using a collective model prescription for the input matrix of interaction potentials, the Pauli exclusion principle can be taken into account by means of the Orthogonalizing Pseudo-Potential (OPP) method [8]. Single-particle and collective-model aspects then can be handled in an single approach for nuclear structure and scattering since both sub-threshold and resonance states of the compound nucleus can be determined.

Originally, the MCAS method was developed and tested in studies with stable light nuclei [3, 7, 9]. Subsequently the method was developed further to infer properties of a light nucleus that is outside of the proton drip line [5]. Crucial to the outcome was the introduction of a new concept which combines collectivity and single-particle dynamics, namely *Pauli hindrance*. This accounts for the fact that the transition from Pauli-allowed to Pauli-blocked single-particle orbits in shell-model structures is not a binary jump but might change gradually with mass. The description in terms of the OPP entails the non-local effects of nucleon state antisymmetrization, and appears perfectly suited parametrically to describe a smooth transitional situation [5].

In the following section, features of the MCAS method and of the properties assumed

for the target nuclei are discussed. This section also includes use of the MCAS method to analyze the spectra of ${}^7\text{Li}$ and of ${}^7\text{Be}$ as dicluster systems of $\alpha+{}^3\text{H}$ and $\alpha+{}^3\text{He}$ respectively. A dicluster-model potential is generated that describes bound and resonance states. The elastic scattering cross sections of the cluster pair for energies to 14 MeV are presented and discussed in that section as well. Thereafter, in Sec. III, the results of our calculations of the coupled-channel problems of a nucleon with a mass-6 nucleus are given and compared with the known spectra of the mass-7 isobars. Finally, in Sec. IV, we give conclusions that may be drawn.

II. THE MCAS THEORY AND SOME STRUCTURE DETAILS

As all details of the MCAS theory have been presented previously [3], only salient features are reviewed herein.

A. Application of MCAS to a nucleon-nucleus coupled-channel system

We use a simple collective-model prescription for the matrix of interaction potentials between a proton and ${}^6\text{He}$, similar to that used previously [3, 7, 8], taking just a quadrupole deformation (deformation parameter β_2) with a mix of central (0), spin-orbit (ls), l^2 (ll), and spin-spin (Is) potential terms, and a Coulomb potential from a uniformly charged sphere of radius R_c , *viz.*

$$V_{cc'}(r) = V_0 v_{cc'}^{(0)}(r, \beta_2) + V_{ls} v_{cc'}^{(ls)}(r, \beta_2) \\ + V_{ll} v_{cc'}^{(ll)}(r, \beta_2) + V_{Is} v_{cc'}^{(Is)}(r, \beta_2) + \delta_{cc'} V_{coul}(r, R_c). \quad (1)$$

The channel index identifies the coupling of specific nucleon partial waves to specific target states leading to each considered, and conserved, total spin-parity J^π of the compound system, *viz.* $c \equiv [(l\frac{1}{2}) jI : J]$, with parity $(-1)^l$ since we consider only positive-parity target states in these applications. It is important to note that the channel indices c incorporate all relevant quantum numbers for a given single-particle state.

The model takes into account effects of core excitation and polarization by allowing transitions from the ground state to the lowest two excited states which are assumed to have collective nature. Therefore, to define the channel space, we assume that there are three important states to consider in the spectrum of ${}^6\text{He}$. They are the 0^+ ground, a 2_1^+ (1.78 MeV) first excited, and a 2_2^+ (5.6 MeV) second excited states. The ground and first excited states of ${}^6\text{He}$ have been given those spin assignments [10], while the third is that expected by a shell-model calculation [1]. Further, for simplicity, we consider transitions between them to be effected by one and the same quadrupole operator though, in expansions, we take the quadrupole deformation to second order [3]. The basic functional form of the channel-coupling interactions is of Woods-Saxon type.

Starting from this local form in coordinate space, the full nuclear potential \mathcal{V} contains, in addition, the highly nonlocal OPP term. The final form is

$$\mathcal{V}_{cc'}(r, r') = V_{cc'}(r)\delta(r - r') + \lambda_c A_c(r)A_c(r')\delta_{cc'}. \quad (2)$$

The function $A_c(r)$ represents the normalized radial part of the single-particle bound state in channel c , spanning the phase-space excluded by the Pauli principle. The OPP method for

treating the effects of the Pauli-blocked states holds in the limit $\lambda_c \rightarrow \infty$, but it suffices to set $\lambda_c = 1000$ MeV to get a stable spectrum where all forbidden states have been removed. For Pauli-allowed states $\lambda_c = 0$. Pauli-hindered states are assumed when specific strengths of λ_c are selected, greater than zero but much lower than 1 GeV and typically a few MeV. Those strengths (λ_c) presently are treated as free parameters.

B. Aspects of structure

If we consider ${}^6\text{He}$ from the point of view of the simplest vibrational model, the two excited states are assumed, respectively, to be a one-phonon and a two-phonon excitation (both with $L=2$) from the ground. As a consequence, and allowing for the scale factor (of 2) that differentiates basic probability expressions for one-phonon couplings between the states, this simple model predicts

$$\begin{aligned} B(E2; 2_2^+ \rightarrow 2_1^+) &= 2 B(E2; 2_1^+ \rightarrow \text{g.s.}) \\ B(E2; 2_2^+ \rightarrow \text{g.s.}) &= 0 . \end{aligned}$$

Neither are close to most observed results as, empirically,

$$0.5 \leq \mathcal{R} = \frac{B(E2; 2_2^+ \rightarrow 2_1^+)}{B(E2; 2_1^+ \rightarrow \text{g.s.})} \leq 1.6 . \quad (3)$$

Wave functions for ${}^6\text{He}$ have been obtained from a complete $(0 + 2 + 4)\hbar\omega$ shell-model calculation [1] in which the G -matrix interactions of Zheng *et al.* [11] were used. This no-core model gave a spectrum with three low-lying states coinciding with the known 0^+ ground and the two excited (resonant) states having centroids at 1.797 and 5.6 MeV. Of those the 1.797 MeV has been assigned 2^+ while the 5.6 MeV resonance is listed [10] with ambiguous spin-parities of $(0^+, 1^-, 2^+)$. The shell model, as noted previously, anticipates 2_2^+ . All three states are radioactive with the 1.797 MeV state having a width of 113 keV. The width of the 5.6 MeV state is uncertain. Other excited states are listed but lie much higher in excitation [10], above 14 MeV.

Using bare charges and oscillator wave functions with an oscillator length of 1.8 fm, the no-core shell model gave $B(E2)$ values for γ -decays in ${}^6\text{He}$ of

$$\begin{aligned} B(E2; 2_1^+ \rightarrow \text{g.s.}) &= 0.153 \text{ e}^2\text{fm}^4 \\ B(E2; 2_2^+ \rightarrow 2_1^+) &= 0.099 \text{ e}^2\text{fm}^4 \\ B(E2; 2_2^+ \rightarrow \text{g.s.}) &= 0.036 \text{ e}^2\text{fm}^4 . \end{aligned}$$

Thus this shell-model calculation of ${}^6\text{He}$ gives a ratio $\mathcal{R} = 0.647$. This lies near the lower limit of the empirical ratio range. Also the shell model predicts that the 2_2^+ state decays to the ground with a significant probability (23.5% of that of the 2_1^+ state).

The isospin mirror, ${}^6\text{Be}$, is particle unstable (decaying to an α and two protons) and from the TUNL Data-Group project [10] it is thought to have a resonant 0^+ ground state and a first excited one, possibly 2^+ , centered 1.7 MeV above. Nonetheless we take for ${}^6\text{Be}$ the same shell-model spectroscopy of ${}^6\text{He}$, under the assumption of charge symmetry of the nuclear force. Thus we assume a second 2^+ excitation, centered around 5.6 MeV, also for the ${}^6\text{Be}$ isotope. In the present analysis we treat all nuclear (target) states, either ground or excited,

TABLE I: Parameter values of the (negative parity) p - ${}^6\text{He}$ interaction.

Strengths	V_0	$V_{\ell\ell}$	$V_{\ell s}$	V_{I_s}
	-36.817	-1.2346	14.9618	0.8511
Geometry	R_0 fm;	a fm;	R_c fm;	β_2
	2.8	0.88917	2.0	0.7298

as stable. In the MCAS scheme unstable states could be accommodated in the formalism. We plan to do so in the near future. Of course the Coulomb interactions used in MCAS calculations take into account the change from 2 to 4 protons and the OPP term refers to states forbidden in the corresponding mirror system. The Coulomb radius was increased to 2.8 fm in this case as well.

As the shell-model calculations give for ${}^6\text{He}$ (and of ${}^6\text{Be}$) comparable admixtures of pair re-coupling and pair breaking in the two 2^+ states, in the collective model prescription of the input matrix of interaction potentials, we have taken the two excitations to be equal mixtures of first and second order terms in the quadrupole-deformation parameter. The deformation β_2 is allowed to be a variable parameter, to be adjusted along with the other parameters of the model interaction to best reproduce the known ${}^7\text{Li}$ spectrum.

We have also performed a shell-model calculation for ${}^7\text{Li}$ using the G -matrix shell-model interaction of Zheng *et al.* [11]. The negative parity states were calculated within a complete $(0 + 2 + 4)\hbar\omega$ model space, as was previously published [12], while the positive parity states were obtained using a $(1 + 3 + 5)\hbar\omega$ model space. The only restriction in the latter was the exclusion of the $5\hbar\omega$ 1p-1h components connecting the $0p$ shell to the $0i-1g-2d-3s$ shell. The shell-model code OXBASH [13] was used for all the calculations from which states up to, and including $J = \frac{7}{2}$, were obtained. We will present and discuss later the results in comparison with those we obtain using MCAS.

Of course, there are many other models for the structure of these nuclei and of ${}^7\text{Li}$ in particular; no-core shell models [14] other than that we have used, Green's function Monte Carlo studies [15], and cluster model investigations [16] to state a few. We also stress the complementary nature of these methods. Cluster and shell-model studies are suitable, in general, for analyses of different data, yet they can also give consistent descriptions of many nuclear properties, as has been pointed out recently [17]. That consistency is evident when one compares the electron scattering form factors for ${}^7\text{Li}$ deduced from a cluster model [16] and from a no-core-shell-model calculation [12]. Those models provide equivalently good fits to data to 2 fm^{-1} .

Recently [18], a dicluster model of ${}^7\text{Li}$ was used to study electromagnetic properties and break-up. The α - ${}^3\text{H}$ system is a single channel problem given the spectra of the two nuclei involved. To reproduce the experimental energies of the four states in ${}^7\text{Li}$ considered, the interaction strengths were adjusted in calculation of the p -wave and f -wave functions of relative motion separately. With those wave functions a variety of data could be described [18]; most of which data are sensitive primarily to the large radius properties of the wave functions. In the following subsection, we develop a similar dicluster-model calculation that reproduces the subset of mass-7 energy levels that significantly couples to the cluster channel.

C. Application to the mass-7 dicluster systems

With the MCAS scheme, we have performed an equivalent dicluster calculation, identifying the dicluster problem as a single-channel potential problem. We have ascertained a single potential that gives a set of compound states in good agreement with some of those in the spectrum of ${}^7\text{Li}$ [10]. The MCAS calculations were made without OPP. As a consequence, there are two deeply bound spurious states which have to be neglected. This is not an essential problem in single-channel studies as, by construct, they are orthogonal to the other excited states. When one considers a coupled-channel problem, however, that is no longer true and due care of the Pauli principle is needed to ensure that all determined states have no spurious components [8]. Later we will incorporate a positive-parity interaction to analyze scattering data. With that interaction, there are also spurious sub-threshold positive-parity states in the evaluated ${}^7\text{Li}$ spectrum. There are three such states of spin-parity $\frac{1}{2}^+$, $\frac{3}{2}^+$, and $\frac{5}{2}^+$, having energies of -11.1 , -6.8 , and -9.0 MeV relative to the $\alpha+{}^3\text{H}$ threshold for the interaction we have determined. These are indeed spurious as there is no known positive parity state in the spectrum below at least 11 MeV excitation [10].

We first discuss results obtained using an α - ${}^3\text{H}$ potential acting only in negative-parity states. A standard Woods-Saxon form [3] was used with parameter values

$$\begin{aligned} V_0 &= -76.8 \text{ MeV} & V_{ll} &= 0.6 \text{ MeV} & V_{ls} &= 1.7 \text{ MeV} \\ R_0 &= 2.39 \text{ fm} & a &= 0.68 \text{ fm} & R_c &= 2.34 \text{ fm} \end{aligned} \quad (4)$$

R_c is the radius of a Coulomb sphere of charge. As the *alpha*-particle is treated solely as a 0^+ state in this model, $V_{l.s} = 0$. For reference later, we define this (purely negative-parity) interaction as Potential I. This was the form that we found best reproduced the known energies of the four physical states of interest in ${}^7\text{Li}$. Their values and resonance widths are given in Table II. It is important to note that, with the dicluster model, there are no other

TABLE II: Spectral properties of ${}^7\text{Li}$ found using Potential I in the MCAS calculation of the $\alpha+{}^3\text{H}$ system. The energies (center of mass, MeV) are relative to the α - ${}^3\text{H}$ threshold. The widths, given in brackets, are in keV.

J^π	Exp.	Potential I
$\frac{3}{2}^-$	spurious	-29.4
$\frac{1}{2}^-$	spurious	-27.8
$\frac{3}{2}^-$	-2.47	-2.47
$\frac{1}{2}^-$	-1.99	-1.75
$\frac{7}{2}^-$	2.18 (60)	2.12 (83)
$\frac{5}{2}^-$	4.13 (918)	4.17 (834)

negative-parity states. But within the low-energy excitation range, a number of other states are known experimentally [10].

1. α scattering from ${}^3\text{H}$

Cross sections at select center of mass scattering angles from the elastic scattering of α -particles from a ${}^3\text{H}$ target for energies between 4 and 13.2 MeV have been measured and

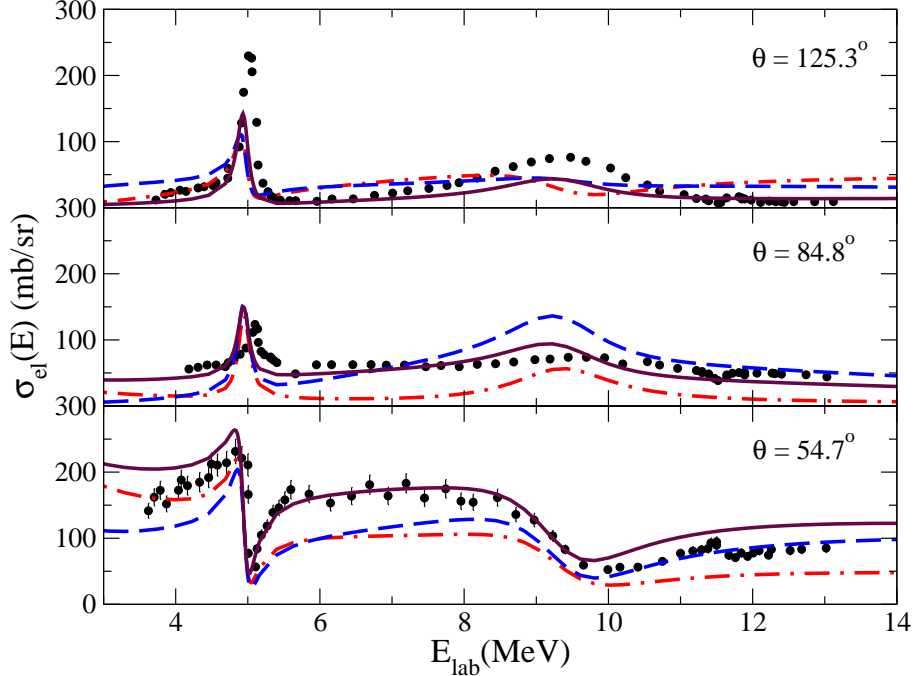


FIG. 1: (Color online) Cross sections from ${}^3\text{H}(\alpha, \alpha){}^3\text{H}$ at the center of mass scattering angles listed. Results differ by various amounts of positive-parity contributions as described in the text.

a phase-shift analysis made [19]. Three resonances were noted, with the phase-shift analysis showing that the $\frac{7}{2}^-$ and first $\frac{5}{2}^-$ states were built from the relative f -wave while the third, a weaker $\frac{5}{2}^-$, was built from the relative p -wave in the scattering. In sequence, their centroids were put at lab. energies of 5.2, 9.8, and ~ 11.5 MeV which link to the known state values in ${}^7\text{Li}$ at 4.65, 6.60 and 7.45 MeV excitation. The first two correspond to the 2.18 and 4.13 MeV states in respect to the α - ${}^3\text{H}$ threshold.

As there are no known positive-parity states in the spectrum of ${}^7\text{Li}$, one can only rely upon scattering data to assess the positive-parity α - ${}^3\text{H}$ interaction. In Fig. 1, a set of results are given for three designated scattering angles at which data have been obtained [19]. Results found using the Potential I interaction (no positive-parity interaction) are displayed by the dot-dashed curves. The dashed curves depict results found with Potential I and assuming that the negative- and positive-parity parameters are the same. The solid curves result when that positive-parity central strength is reduced to -70 MeV, which interaction we identify hereafter as Potential II.

At the scattering angle of 54.7° the cross section found using Potential II reproduces the data well at least to 10 MeV. It is interesting to observe that a decrease in strength of the positive-parity interaction actually enhances the cross-section results to achieve a good comparison with data. This is a signature of strong interference effects between partial-wave contributions. Preference for Potential II is also confirmed by the results at the other scattering angles.

TABLE III: Spectral properties found using the model Potential I in the MCAS method for the ${}^7\text{Be}$ spectra from the $\alpha+{}^3\text{He}$ system. The energies (center of mass, MeV) are relative to the α - ${}^3\text{He}$ threshold. The widths are in keV.

J^π	Exp.	Potential I
$\frac{3}{2}^-$	spurious	-28.0
$\frac{1}{2}^-$	spurious	-26.4
$\frac{3}{2}^-$	-1.59	-1.53
$\frac{1}{2}^-$	-1.16	-0.84
$\frac{7}{2}^-$	2.98 (175)	3.07 (180)
$\frac{5}{2}^-$	5.14 (1200)	5.09 (1194)

2. The case of $\alpha + {}^3\text{He}$ and ${}^7\text{Be}$

Assuming charge symmetry and changing only the Coulomb-force details, we have used Potential I to describe the states of ${}^7\text{Be}$. We have also changed the Coulomb radius to 2.39 fm. That change has minimal impact. Comparison with known state energies [10] is given in Table III. The energies of three of the four low lying states of ${}^7\text{Be}$ are found within 100

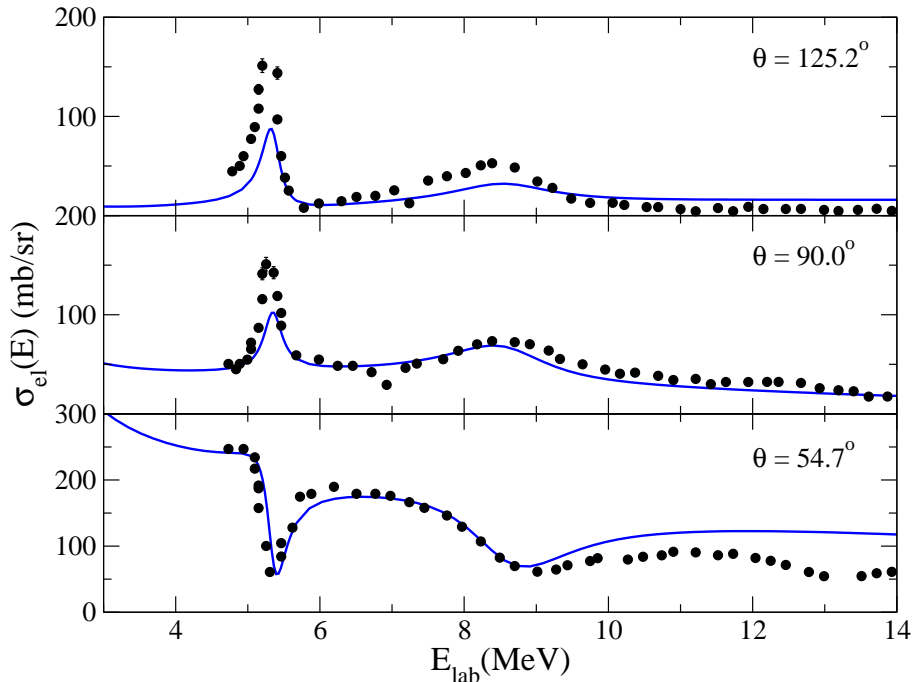


FIG. 2: (Color online) Cross sections from $\alpha({}^3\text{He},{}^3\text{He})\alpha$ at the center of mass scattering angles listed. The curves are predictions made using the Potential II as the inter-nuclear interaction.

keV of the experimental values and the fourth, the $\frac{1}{2}^-$ state, within 320 keV. Even better

are the widths for the two resonance levels being found to within 6 keV. Then we used the MCAS results with Potential II to form elastic scattering cross sections at three center of mass scattering angles ($54.7^\circ, 90.0^\circ, 125.2^\circ$) at which data has been taken [19]. The results of those calculations are shown by the solid curves in Fig. 2. The comparisons with data are very good, adding confirmation to our definition of the basic dicluster-interaction potential.

III. RESULTS OF NUCLEON+MASS-6 NUCLEI CALCULATIONS

Now we return to the description of $A = 7$ nuclei in terms of a nucleon plus mass-6 systems. The ground state energies of the four nuclei of interest, ${}^7\text{He}$, ${}^7\text{Li}$, ${}^7\text{Be}$, and ${}^7\text{B}$ lie at 0.445, -9.975 , -10.676 , and 2.21 MeV with respect to the relevant nucleon-emission thresholds.

The known spectrum of ${}^7\text{Li}$ [10] consists exclusively of negative-parity states so that provides no information on the even-parity interactions. In fact, all mass-7 isobars have only negative-parity entries in their measured spectra up to the excitation energy studied. Since the MCAS method also can define scattering, it is hoped that low-energy ${}^6\text{He}$ ion scattering from hydrogen may soon be measured experimentally, not only to ascertain resonances but also as the average scattering cross section will be sensitive to the positive-parity interaction in the $p+{}^6\text{He}$ system, just as we have found using our dicluster-model potential. It is due to this lack of experimental information that we restrict consideration hereafter to just the effects of the odd-parity interaction.

That all the states are of negative parity may be understood in the simplest shell picture as being dominantly a capture of a $0p$ shell nucleon upon the target states. To form a positive-parity state one has to have capture in the $1s-0d$ shells which requires $1\hbar\omega$ additional energy. For these nuclei, that would be 10 MeV or greater. The $0s$ shell is taken to be fully occupied and so no capture can be made into it. Thus, in the MCAS approach for the mass-7 isobars, the $0s$ shell is to be explicitly Pauli-blocked. This is achieved by the OPP containing a term that prevents further proton- and neutron-occupancies in the $0s$ configurations of the cores.

All results that we present here have been produced with the potential parameter set given in Table I. The components of the potentials are identified in the first line of this table, and their strengths, in MeV, are given in the second. The third line identifies the geometry parameters whose values are listed in the last line. Of the eight parameters of the table, the effective nucleon-nucleus radius R_0 and the corresponding charge radius R_c has been set consistently with shell-model information of ${}^6\text{He}$, corrected due to the size of the (impinging) proton. The remaining 6 parameters have been varied as fit parameters to reproduce 6 out of the 11 known states of ${}^7\text{Li}$, 8 of which are stable with respect to proton emission.

The fit procedure gave a deformation parameter $\beta_2 = 0.7298$. This is a large deformation, more than twice that inferred by using the shell-model $B(E2)$ to determine a collective model value. The diffusivity is larger than typically found with scattering from stable nuclei, but that may simply reflect the neutron halo character of ${}^6\text{He}$. The spectrum found from the MCAS evaluations of the $p+{}^6\text{He}$ system is compared in Table IV with the experimentally known spectrum of ${}^7\text{Li}$ [10]. Therein we also give the results obtained for the mirror case, ${}^7\text{Be}$, which has been treated in the MCAS formalism as an $n+{}^6\text{Be}$ system. The energies are in MeV but the widths, shown in brackets, are in keV. The numbers in square brackets are the corresponding experimental widths with respect to the $t+\alpha$ channel for ${}^7\text{Li}$, and ${}^3\text{He}+\alpha$ channel for ${}^7\text{Be}$. Also the decay into the channels $n-{}^6\text{Li}$ and $p-{}^6\text{Li}$ are included,

TABLE IV: Experimental data and theoretical results for ${}^7\text{Li}$ and ${}^7\text{Be}$ states (Energies are in MeV, widths are in keV). All energies are defined with thresholds, $p+{}^6\text{He} = 9.975$ MeV with respect to ${}^7\text{Li}$ ground state and $n+{}^6\text{Be} = 10.676$ MeV with respect to ${}^7\text{Be}$ ground state.

J^π	${}^7\text{Li}$		${}^7\text{Be}$	
	Exp.	Theory	Exp.	Theory
$\frac{3}{2}^-$	-9.975	-9.975	-10.676	-11.046
$\frac{1}{2}^-$	-9.497	-9.497	-10.246	-10.680
$\frac{7}{2}^-$	-5.323 [69]	-5.323	-6.106 [175]	-6.409
$\frac{5}{2}^-$	-3.371 [918]	-3.371	-3.946 [1200]	-4.497
$\frac{3}{2}^-$	-2.251 [80]	-0.321	-3.466 [400]	-1.597
$\frac{3}{2}^-$	-1.225 [4712]	-2.244	--	--
$\frac{1}{2}^-$	-0.885 [2752]	-0.885		-2.116
$\frac{7}{2}^-$	-0.405 [437]	-0.405	-1.406 [?]	-1.704
$\frac{3}{2}^-$	--	--	-0.776 [1800]	-3.346
$\frac{3}{2}^-$	1.265 (260)	0.704 (56)	0.334 (320)	-0.539
$\frac{1}{2}^-$		1.796 (1570)		0.727 (699)
$\frac{3}{2}^-$	3.7 (800) ? ^a	2.981 (990)		1.995 (231)
$\frac{5}{2}^-$	4.7 (700) ? ^a	3.046 (750)		2.009 (203)
$\frac{5}{2}^-$		5.964 (230)		4.904 (150)
$\frac{7}{2}^-$		6.76 (2240)	6.5 (6500) ? ^b	5.78 (1650)

^a For these states spin and parity are unknown [10].

^b Spin-parity of this state has been assigned as $\frac{1}{2}^-$ [10].

respectively, when these channels are open. Above the relevant zero-energy thresholds the experimental widths are indicated in round brackets and are compared with values calculated with MCAS. As the theoretical widths refer only to the specific nucleon decay channels, they differ somewhat in significance with respect to the experimental ones which include other break-up contributions. Our evaluation produced 12 states to 15 MeV excitation in ${}^7\text{Li}$. The lowest 9 match states match known spin-parity states in the spectrum. while the next three calculated levels are in the energy region in which two resonant states of undetermined spin-parity are known. The matched states agree quite well in energies save for a crossing of the $\frac{3}{2}^-|_2$ with the $\frac{5}{2}^-|_2$ states. A measure of the quality of result is that the mean square error, calculated over the 8 states in ${}^7\text{Li}$ below the proton emission threshold, is

$$\mu = \frac{1}{N} \sqrt{\sum (E_{th} - E_{exp})^2} = 0.2728 \text{ MeV}. \quad (5)$$

By including the resonances, assuming the assignments, the mean square error remains good, namely $\mu = 0.2966$ MeV. Also the agreement between widths for the resonances is satisfactory given that no adjustments have been made to get a better fit to them. But the experimental widths have various components. The ground state in ${}^7\text{Li}$ is stable and the first excited decays only electromagnetically. The next two can decay also by emission of a triton or an α particle as the threshold for that decay is 2.467 MeV above the ${}^7\text{Li}$ ground state value. The next states in the spectrum can also decay by neutron emission as the $n+{}^6\text{Li}$ threshold lies 7.25 MeV above ${}^7\text{Li}$ ground.

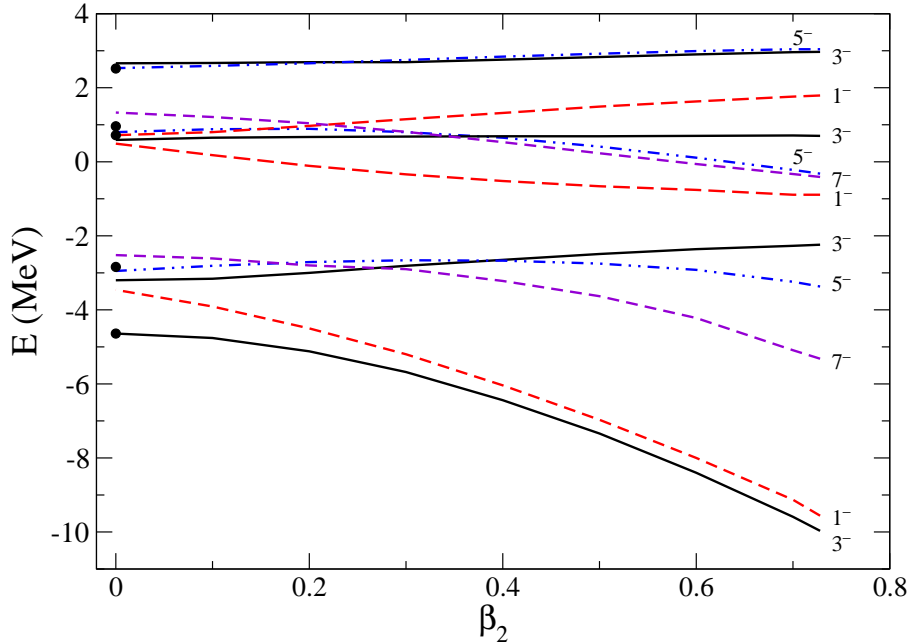


FIG. 3: (Color online) The calculated energy spectrum of ${}^7\text{Li}$ as β_2 varies.

To interpret the structure of the evaluated spectra, we follow the procedure used previously [7, 8] of allowing the deformation to decrease to zero. The variation of the spectrum is shown in Fig. 3. Each state is identified on the right by twice its spin and its parity. The dots show the degenerate spectrum values when $\beta_2 = V_{I_s} = 0$. States cluster as the deformation vanishes with the residual separation of groups due to the effect of the (target)spin-(proton)spin interaction V_{I_s} being finite. Evidently, the individual states retain an element of their zero deformation grouping for all of them track smoothly with β_2 and do not cross any member of another group. Some states within each group do cross (interchange their order in the spectrum as β_2 decreases) when β_2 lies in the range 0.2 to 0.35. Nevertheless, the mixing of basis states is evident from the rapid divergence of the members of the two primary groups with increasing β_2 .

Setting that interaction strength $V_{I_s} = 0$ at zero deformation gives the spectrum of degenerate states shown in the leftmost column of Fig. 4. The states are identified by their value of $(2 \times \text{spin})$ -parity. The mapping of our results against the experimental spectrum discussed above is clear on comparing the central (theoretical) against the empirical (rightmost) spectra. Comparing now with the zero deformation results, it is clear that the dominant term in the ground state specification is the coupling of a $0p_{\frac{3}{2}}$ proton to the ground state of the target. Of course with deformation non-zero, the actual description is a linear combination of all such basis $\frac{3}{2}^-$ states. The next four states in the spectrum dominantly are formed by coupling a $0p_{\frac{3}{2}}$ proton to the first excited 2^+ state of the target as the energy gap in the unperturbed spectrum is 1.78 MeV. The next state with spin-parity $\frac{1}{2}^-$ is a member of the quartet of states built primarily from the coupling of a $0p_{\frac{3}{2}}$ proton to the second excited 2^+ state of the target. Then there is another $\frac{1}{2}^-$ state which resolves to the unique coupling of a $0p_{\frac{1}{2}}$ proton with the ground state when the deformation vanishes. Its energy (0.73 MeV) in that limit lies 5.36 MeV above the ground state value and that is the spin-orbit splitting of the single proton states in this model. Finally there is the doublet of states formed by coupling a $0p_{\frac{1}{2}}$ proton to the first excited 2^+ state of the target. Confirmation of these assignments comes from tracking the widths of resonances found as β_2 decreases.

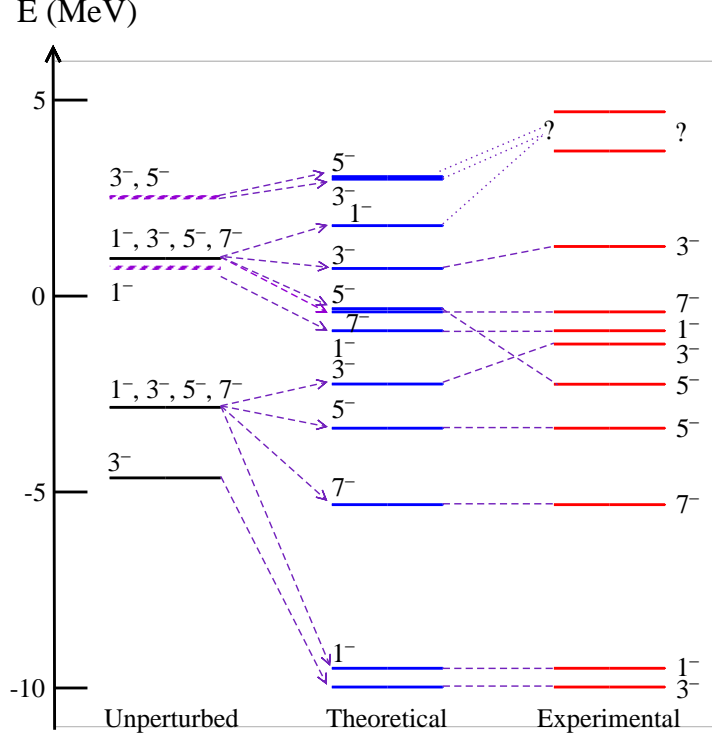


FIG. 4: (Color online) The calculated energy spectrum of ${}^7\text{Li}$ compared to the experimentally known one. The left column is the zero deformation and $V_{I_s} = 0$ result. Spin-parities to the top most experimental levels have not been assigned

For those states that are in, or move into, the continuum with decreasing β_2 , their centroids and widths are given in Table V. In this, the subscript n designates the rank of the state in the theoretical spectrum, while the letter ‘m’ in the brackets, which otherwise contains the width, signifies a value less than 1 eV. Usually it is much less than that. The quartet

TABLE V: Centroids (MeV) and widths (keV) of resonance states in ${}^7\text{Li}$ as β_2 decreases.

$J^\pi n$	β_2 for ${}^7\text{Li}$							
	0.7	0.6	0.5	0.4	0.3	0.2	0.1	0.0
$\frac{1}{2} 2$							0.18 (1)	0.49 (m)
$\frac{7}{2} 2$			0.23 (m)	0.53 (m)	0.81 (m)	1.04 (m)	1.21 (m)	1.33 (m)
$\frac{5}{2} 2$		0.11 (m)	0.41 (m)	0.65 (m)	0.82 (m)	0.89 (m)	0.80 (m)	0.80 (m)
$\frac{3}{2} 3$	0.71 (54)	0.70 (42)	0.69 (30)	0.69 (18)	0.68 (10)	0.67 (4)	0.65 (m)	0.59 (m)
$\frac{1}{2} 3$	1.76 (1510)	1.63 (1303)	1.49 (1180)	1.32 (858)	1.15 (652)	0.97 (652)	0.80 (334)	0.72 (418)
$\frac{3}{2} 4$	2.96 (900)	2.90 (848)	2.83 (780)	2.76 (680)	2.69 (652)	2.65 (600)	2.63 (580)	2.66 (610)
$\frac{5}{2} 3$	3.04 (740)	2.99 (700)	2.92 (646)	2.84 (584)	2.75 (526)	2.66 (480)	2.59 (440)	2.53 (398)

of states, all having widths less than 1 eV, coincide with the zero deformation and $V_{I_s} = 0$ degenerate set having an energy of 0.96 MeV. They are built upon a single particle bound in the continuum. The $\frac{1}{2}^-$ state that tends to 0.724 MeV, and the doublet that tends to a degenerate value of 2.52 MeV, are built upon single particle resonances in the continuum

TABLE VI: Experimental data and theoretical results for ${}^7\text{He}$ and ${}^7\text{B}$ states. All energies are in MeV and relate to thresholds of -0.445 MeV for $n+{}^6\text{He}$ and of -2.21 MeV for $p+{}^6\text{Be}$.

J^π	${}^7\text{He}$		${}^7\text{B}$	
	Exp.	Theory	Exp.	Theory
$\frac{3}{2}^-$	0.445 (150)	0.43 (100)	2.21 (1400)	2.10 (190)
$\frac{7}{2}^-$	--	1.70 (30)		3.01 (110)
$\frac{1}{2}^-$	1.0 (750) ? ^a	2.79 (4100)		5.40 (7200)
$\frac{5}{2}^-$	3.35 (1990)	3.55 (200)		5.35 (340)
$\frac{3}{2}^-$	6.24 (4000) ? ^b	6.24 (1900)		

^a Observed very recently and interpreted as a $\frac{1}{2}^-$ state.

^b Spin-parity of this state is unknown

whose inherent width is 580 keV.

The same nucleon-nucleus matrix of interactions, but with no Coulomb terms, was used to evaluate the spectrum of the isospin mirror system $n+{}^6\text{Be}$. Again in making comparison with the experimental spectra for ${}^7\text{Be}$, one must bear in mind the threshold energies of reactions, ${}^3\text{He} + \alpha$ of 1.586 MeV, $p+{}^6\text{Li}$ of 5.806 MeV, and $n+{}^6\text{Be}$ at 10.676 MeV. Our predicted spectrum of ${}^7\text{Be}$ is compared with the known values also in Table IV and again the round brackets around the calculated widths are solely for neutron emission. The five lowest lying states in the known spectrum compare reasonably with the MCAS values. The calculations give more states than are known to date above an excitation energy of ~ 8.5 MeV in ${}^7\text{Be}$, and there are a few crossings. But the result is a limited one in that it is predicated upon charge symmetry and the simple collective model prescription. Studies using other model prescriptions are in progress.

The spectrum of ${}^7\text{He}$, so far as it is known experimentally, has three resonant states with only the ground being quite narrow. There is a claim [20] of a fourth resonance $\frac{1}{2}^-$ at $\simeq 1$ MeV above threshold which we include in Table VI. Our calculation puts it higher in energy, as do shell-model calculations. Additionally we find a narrow $\frac{7}{2}^-$ resonance at 1.7 MeV excitation that has not been observed. In the MCAS calculations of the ${}^7\text{He}$ nucleus, one must introduce a Pauli-hindrance effect on the $0p$ shells. This effect produces a ground state that is unbound with respect to neutron emission. Specifically, one must invoke an hindrance of both the $0p_{\frac{3}{2}}$ and $0p_{\frac{1}{2}}$ shells. With this system, such effects might be a reflection of an exotic and non-compact structure (${}^6\text{He}$) being used as a basis in the channel coupling. A similar discussion applies also for a proton coupled to ${}^6\text{Be}$ states. However, only the ground state of ${}^7\text{B}$ is known and it is encouraging that the MCAS calculation has found that resonance energy accurate to 5%. As shown in Tab. VI, we also predict three more resonances, two of which have widths sufficiently narrow to be detected in experiments.

With the same nucleon-nucleus interaction, fixed by properties of ${}^7\text{Li}$, and only modified by a Coulomb field, we describe spectra of two unbound nuclei ${}^7\text{He}$ and ${}^7\text{B}$. The calculations of these differ from those for the isospin mirrors, ${}^7\text{Li}$ and ${}^7\text{Be}$, in regard to the OPP terms. While Pauli blocking of the $0s_{\frac{1}{2}}$ shell is common to all four nuclides, the two particle-unstable ones have additional OPP terms responsible for Pauli hindrance in the $0p_{\frac{3}{2}}$ and $0p_{\frac{1}{2}}$ shells. The parameter λ_c was set as 17.8 MeV for the $0p_{\frac{3}{2}}$ shell in each of the three target states considered, while for the $0p_{\frac{1}{2}}$ shell, λ_c was set as 36.0 MeV for the 0^+ g.s., but as 5.8 MeV

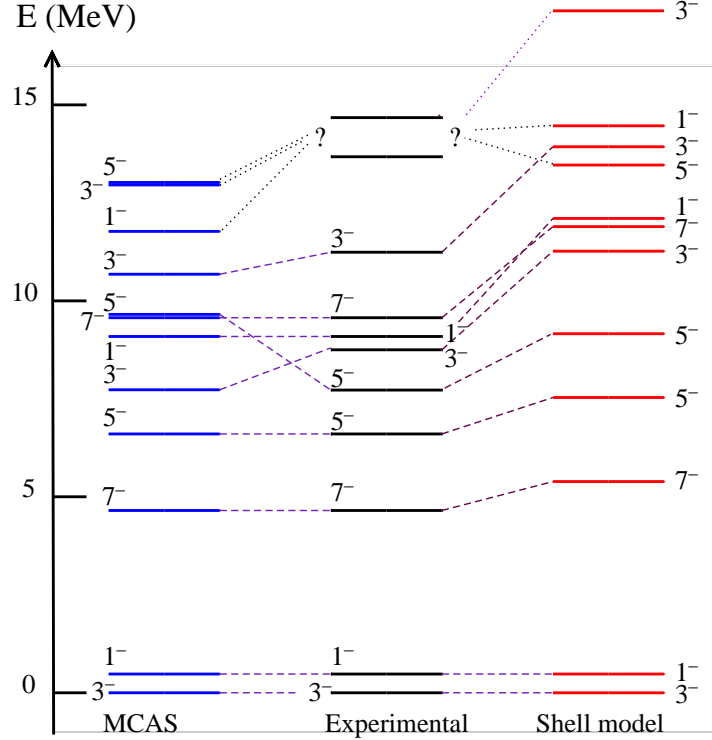


FIG. 5: (Color online) The calculated energy spectra of ${}^7\text{Li}$ compared to the experimentally known one. The left and right columns are the MCAS and the no-core-shell-model results respectively. The known spectrum [10] is given in the middle column.

for the two excited 2^+ states. The same hindrance effects were used for both ${}^7\text{He}$ and ${}^7\text{B}$.

Finally we compare the MCAS results for ${}^7\text{Li}$ with both the known spectrum and with that determined from our no-core-shell-model calculations. Those spectra to 15 MeV excitation are shown in Fig. 5 and each state identified by twice its spin and its parity. In both calculated spectra there is a high lying triplet of states, the $\frac{1}{2}^-|_3$, $\frac{3}{2}^-|_4$, and $\frac{5}{2}^-|_3$ that coincide with a doublet of resonances of unknown spin-parity in the known spectrum [10]. All lower excitation states have defined spin-parity and are paired to ones in both calculated spectra. The shell-model results reproduce the known spectrum [10] quite well and that calculation also found the lowest energy positive parity state to be a $\frac{1}{2}^+$ state at 33.7 MeV excitation. The sequencing of the states in the spectrum given by the shell-model calculation is also very good with one minor cross over of the $\frac{7}{2}^-|_2$ and $\frac{1}{2}^-|_2$ states, and a larger cross over only occurring with the $\frac{5}{2}^-|_3$ at ~ 15 MeV excitation. As noted there is a 1:1 correspondence between states in the MCAS and shell-model spectra with the MCAS spectra (of states not used in determination of the $V_{cc}(r)$) being slightly compressed while the shell-model spectra is slightly expanded in energies in comparison to the known states. This, we believe could be evidence of the need for more collectivity in the shell-model description and a softening of that given by MCAS.

IV. CONCLUSIONS

We have used a collective-model prescription of a three-state (0^+ ground, 2_1^+ , and 2_2^+) spectrum for the isospin-mirror nuclei, ${}^6\text{He}$ and ${}^6\text{Be}$, in forming the coupling interactions with an extra nucleon to yield the bound and resonant spectra of the mass-7 isobars. We used only a quadrupole deformation but chose parameters consistent with the mass-6 targets having extended (halo) nucleon distributions. We have also used a dycluster-model potential to assess states in ${}^7\text{Li}$ and ${}^7\text{Be}$ that can have strong coupling in the cluster-cluster channels, ${}^3\text{H}+\alpha$ and ${}^3\text{He}+\alpha$. The first four levels of the nuclei are well reproduced as are the widths of the f -wave resonances. With this interaction, the low-energy elastic scattering cross sections of the clusters are also well reproduced. However, the dycluster model gives no other state in the spectra, while a number of other states have been observed. In contrast, a complete reproduction of the bound and resonance levels for all mass-7 isobars was found from the coupled-channel solutions of the nucleon-mass-6 systems when a single, fixed, nucleon-nucleus interaction was used. Specifically we found very good reproductions of the spectra of the stable isobars, ${}^7\text{Li}$ (from $p+{}^6\text{He}$) and ${}^7\text{Be}$ (from $n+{}^6\text{Be}$). The other two isobars, ${}^7\text{He}$ (from $n+{}^6\text{He}$) and ${}^7\text{B}$ (from $p+{}^6\text{Be}$) are, as known [10], particle unstable. The MCAS predictions for their (resonant) ground states is consistent with the available data once Pauli-hindrance in the $0p$ shells is invoked. Other yet to be discerned resonances are predicted, suggesting a complex scenario of low-lying odd-parity resonances.

Acknowledgments

This research was supported by the Italian MIUR-PRIN Project “Struttura Nucleare e Reazioni Nucleari” and by the Natural Sciences and Engineering Research Council (NSERC), Canada. K. A. and D. v.d. K. gratefully acknowledge the support and hospitality of the I.N.F.N. (section Padova) and the University of Padova during visits in which this research was developed, as do L. C. and J. P. S. for that given by the University of Melbourne during their visits.

-
- [1] S. Karataglidis, P. J. Dortmans, K. Amos, and C. Bennhold, *Phys. Rev. C* **61**, 024319 (2000).
 - [2] S. Stepantsov et al., *Phys. Lett.* **542**, 35 (2002).
 - [3] K. Amos, L. Canton, G. Pisent, J. P. Svenne, and D. van der Knijff, *Nucl. Phys.* **A728**, 65 (2003).
 - [4] K. Amos, P. J. Dortmans, H. V. von Geramb, S. Karataglidis, and J. Raynal, *Adv. in Nucl. Phys.* **25**, 275 (2000).
 - [5] L. Canton, G. Pisent, J. P. Svenne, K. Amos, and S. Karataglidis, *Phys. Rev. Lett.* **96**, 072502 (2006).
 - [6] F. Q. Guo et al., *Phys. Rev. C* **72**, 034312 (2005).
 - [7] G. Pisent, J. P. Svenne, L. Canton, K. Amos, S. Karataglidis, and D. van der Knijff, *Phys. Rev. C* **72**, 014601 (2005).
 - [8] L. Canton, G. Pisent, J. P. Svenne, D. van der Knijff, K. Amos, and S. Karataglidis, *Phys. Rev. Lett.* **94**, 122503 (2005).

- [9] J. P. Svenne, K. Amos, S. Karataglidis, D. van der Knijff, L. Canton, and G. Pisent, Phys. Rev. C **73**, 027601 (2006).
- [10] D. R. Tilley, C. M. Cheves, J. L. Godwin, G. M. Hale, H. M. Hoffman, J. H. Kelley, C. G. Sheu, and H. R. Weller, Nucl. Phys. **A708**, 3 (2002).
- [11] D. C. Zheng, B. R. Barrett, J. P. Vary, W. C. Haxton, and C.-L. Song, Phys. Rev. C **52**, 2488 (1995).
- [12] S. Karataglidis, B. A. Brown, K. Amos, and P. J. Dortmans, Phys. Rev. C **55**, 2826 (1997).
- [13] A. Etchegoyen, W. D. M. Rae, and N. S. Godwin, *OXBASH-MSU (the Oxford-Buenos-Aires-Michigan State University shell model code), MSU version by B. A. Brown* (1986).
- [14] A. Nogga, P. Navrátil, B. R. Barrett, and J. P. Vary, Phys. Rev. C **73**, 064002 (2006).
- [15] S. C. Pieper, R. B. Wiringa, and J. Carlson, Phys. Rev. C **70**, 054325 (2004).
- [16] H. Walliser and T. Fließbach, Phys. Rev. C **31**, 2242 (1985).
- [17] L. Zamick and S. J. Q. Robinson, Phys. Atom. Nucl. **65**, 740 (2002).
- [18] L. Fortunato and A. Vitturi, Eur. Phys. J. **A26**, 33 (2005).
- [19] R. J. Spiger and T. A. Tombrello, Phys. Rev. **163**, 964 (1967).
- [20] M. Meister et al., Phys. Rev. Lett. **88**, 102501 (2002).